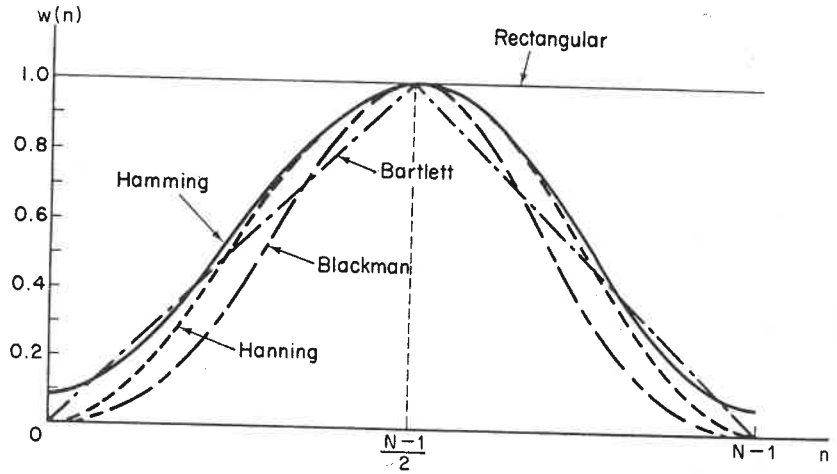

Fig. 5.33 Commonly used windows for FIR filter design.

Hanning:

$$w(n) = \frac{1}{2}\left[1 - \cos\left(\frac{2\pi n}{N-1}\right)\right], \qquad 0 \le n \le N-1 \tag{5.55c}$$

Hamming:

$$w(n) = 0.54 - 0.46\cos\left(\frac{2\pi n}{N-1}\right), \qquad 0 \le n \le N-1 \tag{5.55d}$$

Blackman:

$$w(n) = 0.42 - 0.5\cos\left(\frac{2\pi n}{N-1}\right) + 0.08\cos\left(\frac{4\pi n}{N-1}\right), \qquad 0 \le n \le N-1 \tag{5.55e}$$

The function $20\log_{10}|W(e^{j\omega})|$ is plotted in Fig. 5.34 for each of these windows for $N = 51$. Note that since these windows are all symmetrical, the phase is linear. The rectangular window clearly has the narrowest main lobe and thus, for a given length, N should yield the sharpest transitions of $H(e^{j\omega})$ at a discontinuity of $H_d(e^{j\omega})$. However, the first side lobe is only about 13 dB below the main peak, resulting in oscillations of $H(e^{j\omega})$ of considerable size at a discontinuity of $H_d(e^{j\omega})$. By tapering the window smoothly to zero, the side lobes are greatly reduced; however, it is clear that the price paid is a much wider main lobe and thus wider transitions at discontinuities of $H_d(e^{j\omega})$.

Kaiser [4] has proposed a flexible family of windows defined by

$$w(n) = \frac{I_0\left[\omega_a\sqrt{\left(\frac{N-1}{2}\right)^2 - \left[n - \left(\frac{N-1}{2}\right)\right]^2}\right]}{I_0\left[\omega_a\left(\frac{N-1}{2}\right)\right]} \tag{5.55f}$$

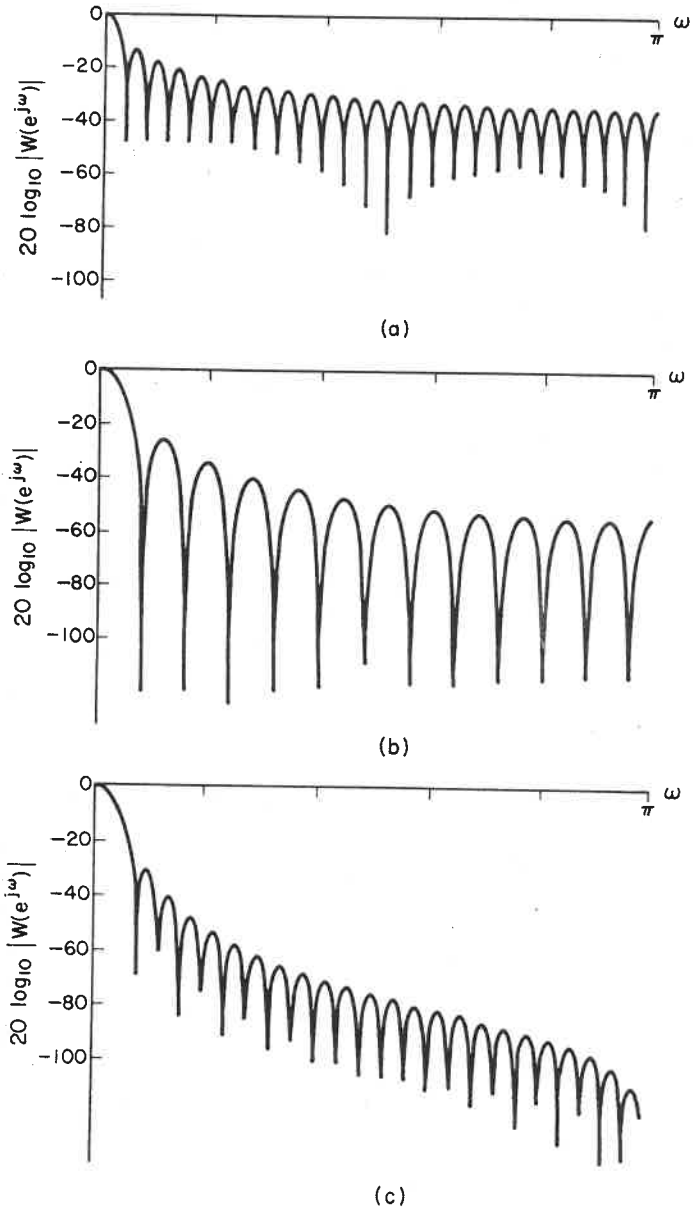

Fig. 5.34 Fourier transforms of windows of Fig. 5.33: (a) rectangular; (b) Bartlett (triangular); (c) Hanning; (d) Hamming; (e) Blackman.

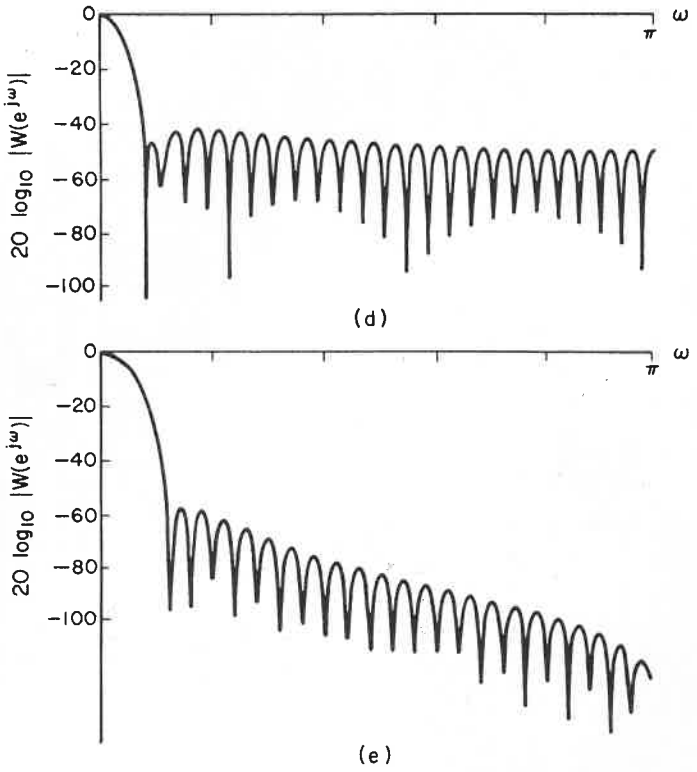

Fig. 5.34 *continued*

where $I_0(\ )$ is the modified zeroth order Bessel function of the first kind. Kaiser has shown that these windows are nearly optimum in the sense of having the largest energy in the main lobe for a given peak side lobe amplitude. The parameter ω_a can be adjusted so as to trade off main-lobe width for side-lobe amplitude. Typical values of $\omega_a((N-1)/2)$ are in the range $4 < \omega_a((N-1)/2) < 9$.

As an illustration of the use of windows in filter design, consider the design of a lowpass filter. Anticipating the need for delay in achieving a causal linear-phase filter, the desired frequency response is defined as

$$H_d(e^{j\omega}) = \begin{cases} e^{-j\omega\alpha}, & |\omega| \le \omega_c \\ 0, & \text{otherwise} \end{cases}$$

The corresponding impulse response is

$$h_d(n) = \begin{cases} \dfrac{1}{2\pi}\displaystyle\int_{-\omega_c}^{\omega_c} e^{j\omega(n-\alpha)}\,d\omega \\ \dfrac{\sin[\omega_c(n-\alpha)]}{\pi(n-\alpha)}, & n \neq \alpha \end{cases}$$

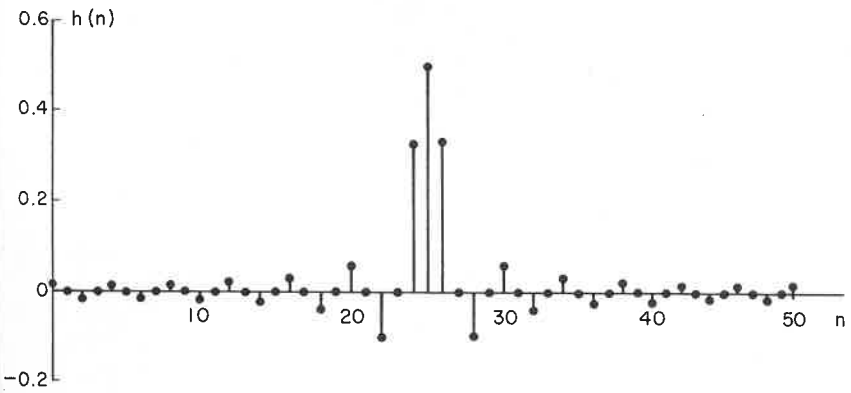

Fig. 5.35 Truncated impulse response of an ideal lowpass filter. (Delay is 25 samples, total length is 51 samples, and cutoff frequency is $\omega_c = \pi/2$.)

Clearly, $h_d(n)$ has infinite duration. To create a finite-duration linear-phase causal filter of length N, we define

$$h(n) = h_d(n)w(n)$$

where

$$\alpha = \frac{N-1}{2}$$

It can be easily verified that if $w(n)$ is symmetrical, this choice of α results in a sequence $h(n)$ satisfying Eq. (5.47). Figure 5.35 shows a plot of $h(n)$ for a rectangular window, $N = 51$, and $\omega_c = \pi/2$. Figure 5.36 shows $20 \log_{10} |H(e^{j\omega})|$ for the impulse response of Fig. 5.35 weighted by each of five windows of Fig. 5.34. Note the increasing transition width, corresponding to increasing main-lobe width, and the increasing stopband attenuation, corresponding to decreasing side-lobe amplitude.

From Eq. (5.54) we note that the width of the central lobe is inversely proportional to N. This is generally true and is illustrated for a Hamming window in Fig. 5.37, where it is clearly evident that as N is doubled, the width of the central lobe is halved. Figure 5.38 illustrates the effect of increasing N on the transition region in a lowpass filter design. Clearly, the minimum stopband attenuation remains essentially constant, being dependent on the shape of the window, while the width of the transition region at the discontinuity of $H_d(e^{j\omega})$ depends on the length of the window.

The examples that we have given illustrate the general principles of the windowing method of FIR filter design. Through the choice of the window shape and duration, we can exercise some control over th sign process.